

**Normalized Microwave Reflection Index:
Validation of Vegetation Water Content Estimates from Montana Grasslands**

Eric E. Small^a, Kristine M. Larson^b, and W. Kolby Smith^c

a Department of Geological Sciences, University of Colorado

UCB 399

2200 Colorado Avenue

Boulder, Colorado, USA 80309

eric.small@colorado.edu *Corresponding author*

303 735 5033

b Department of Aerospace Engineering Sciences, University of Colorado

ECOT-634

Aerospace Engineering Sciences Department

University of Colorado 429 UCB

Boulder, Colorado, USA 80309

Kristinem.larson@gmail.com

c Numerical Terradynamic Simulation Group, Department of Ecosystems and Conservation

Sciences, University of Montana

bill.smith@ntsg.umt.edu

Abstract

The Normalized Microwave Reflection Index (NMRI) measures the intensity of GPS reflections, which is affected by vegetation within ~100 m of GPS antennas. In a companion paper, the theoretical basis for NMRI and how it is derived from data archived at geodetic GPS installations are described. NMRI is calculated by normalizing the standard GPS metric MP_{1rms} on a site-by-

site basis to minimize terrain effects. Here, we validate NMRI as a metric for estimating vegetation water content (VWC) and evaluate the normalization procedure. *In situ* measurements of plant height, biomass, and VWC were taken on a biweekly basis during 2012 at four grassland sites in Montana. These measurements were compared to time series of MP₁rms, NMRI and NDVI from each site. Precipitation was below normal during the 2012 growing season, but vegetation growth was only severely affected at one site. At each site, a significant linear relationship exists between MP₁rms and VWC. However, this relationship is not consistent across sites. Once normalized, a linear relationship exists between NMRI and VWC ($r^2 = 0.71$) that is consistent across the four sites. This suggests that VWC could be predicted from NMRI at sites without *in situ* observations, as long as vegetation and climate are similar. There is no clear relationship between NMRI and either vegetation height or biomass. The importance of normalization is shown using data from eight additional sites in Montana. After normalization, a strong positive correlation is apparent between NMRI and NDVI across all grassland GPS sites in Montana.

1. Introduction

Larson and Small (this issue, hereafter Paper I) introduced the Normalized Microwave Reflection Index (NMRI). It is a measure of vegetation water content (VWC) estimated from data archived by GPS instruments deployed for geodetic applications, such as the 1100 stations in the EarthScope Plate Boundary Observatory (PBO) network. GPS satellites transmit L-band microwave signals; some of this energy is reflected by the surface surrounding the antenna. Small et al. [1] showed that variations in reflectance amplitude were correlated with VWC and vegetation height in irrigated corn and hay fields. Paper I describes the theoretical basis of this

reflectance, how it is impacted by snow and rain, and how the standard GPS noise metric MP_{1rms} [2] is normalized to mitigate topographic effects. This yields a measure of reflectivity (NMRI) that can be used to compare VWC between sites. In this companion paper, we validate NMRI by comparing it with field observations of vegetation biophysical parameters from four grassland sites in Montana.

There is a long history of converting reflectance data from satellite-borne sensors into metrics of ‘greenness’, such as the Normalized Difference Vegetation Index (NDVI) and variants [3], [4]. Greenness is an indicator of photosynthetic activity and has been used to estimate biophysical parameters [5], [6]. Tower-mounted sensors yield equivalent measures of greenness at the hectare scale [7]. Greenness does not completely describe vegetation status – measurements of the amount of water stored in vegetation are also important [8]. VWC can be estimated from optical remote sensing indices, such as Normalized Difference Water Index or related metrics [9], [10]. Alternatively, VWC and related parameters can be estimated from microwave remote sensing data [11]. Tower-mounted microwave radars have been used to estimate VWC at the hectare scale (e.g., [12]). NMRI estimated from GPS data yields a similar microwave-based estimate of VWC.

This study has three goals. First, we describe seasonal fluctuations of NMRI at the four grassland validation sites. NDVI records for the GPS locations are included in our analyses to provide a standard metric against which to compare NMRI performance. Second, we quantify how MP_{1rms} and NMRI vary with VWC, vegetation height, and biomass on a site-by-site basis. Third, we quantify how NMRI varies with these same vegetation parameters across sites. Our analyses provide information on whether or not VWC can be predicted solely from NMRI data, using a relationship derived by comparing field and NMRI observations from elsewhere in the

same ecosystem. Our analyses also demonstrate the importance of normalizing the standard GPS MP_{1rms} data stream. Normalization is required if MP_{1rms} -VWC relationships vary from site to site. Below, we demonstrate that this is the case. Normalization is successful if a consistent relationship exists between NMRI and VWC across sites. We also show that this is the case. We further demonstrate the importance of normalization using NMRI data from eight additional GPS sites in Montana grasslands, for which no *in situ* observations of vegetation state were made. The datasets used in this study are limited to grasslands of the northern plains. Additional data would be needed to assess the transferability of the VWC-NMRI relationship to sites in other ecosystems and climates.

In the next section, the field sites and the field measurement protocol are described. Only limited information is provided regarding the GPS data, as the material is covered in detail in Paper I. In section 3, the climate conditions and vegetation state during the validation period (2012) are described. Then the temporal variations of NMRI with vegetation data at each site are compared individually. This is followed by a comparison of NMRI and field observations across sites. In section 4, we summarize our results and discuss various issues associated with validating and using NMRI data.

2. Field sites and data

2.1 Field sites

We selected four GPS sites from the EarthScope Plate Boundary Observatory (<http://pbo.unavco.org>) in Montana (Figure 1, Table 1) to validate the NMRI product described in Paper I. These sites were chosen based on the following criteria. First, grasslands were selected because this land cover type exhibits clear seasonal variations in NMRI. All four sites

are classified as grassland according to the MODIS MCD12Q1 500-m land cover product using the IGBP classification scheme [13]. Inspection of Google Earth images confirmed that sites were primarily grassland. Second, site access was required to sample vegetation, which is not possible at some GPS sites. And third, the validation sites needed to be close enough together to allow visiting all sites within a two-day sampling trip. We use NMRI data from eight additional GPS sites to supplement the validation of our normalization procedure (Figure 1). Together, these twelve sites represent all PBO sites in Montana where NMRI records are available and land cover is classified as grassland.

Vegetation at the validation sites is characterized by a relatively short growing season that begins in early May and continues until the end of September, due to seasonal temperature and day-length constraints. During the growing season, water availability is the dominant biophysical limitation on growth, generally limiting productivity toward the end of the growing season [14]. Precipitation is not measured at the validation sites. We use two independent datasets to estimate precipitation: (1) daily precipitation from the National Land Data Assimilation System (NLDAS) forcing A data [15]; and (2) monthly precipitation from the PRISM dataset [16]. Mean annual precipitation is between 390 and 520 mm at the sites (Table 1). In 2012, three of the four sites experienced drought conditions, so the limitations due to water availability were likely above-normal during the validation period. This is discussed further in Section 3.1.

2.2 Sensing footprint and heterogeneity of vegetation

The validation sites are dominated by perennial grasses. However, the amount and type of vegetation is not completely uniform within the maximum NMRI footprint (300 m radius) at each site (Figure 2). P046 is the most heterogeneous site. The area south of the antenna is covered exclusively by perennial grasses, but to the north there are also some trees and shrubs

within the maximum sensing footprint. Figure 2 shows the near-antenna reflection zones and the estimated location of reflection ‘hot spots’ for each site. (See Part I for more details on estimation of hot spot locations.) At P046, most of the GPS reflections received are from areas dominated by grasses. However, reflections from the hot spot to the northwest of the antenna may be partly affected by deciduous shrubs and short trees.

Vegetation heterogeneity at P048 (Figure 2) is due to topography and land use. Livestock grazing is more intense to the south of the east-west fence line. Both the near-antenna reflection zone and the reflection hotspot to the northwest of the antenna are located in areas dominated by grasses. Even so, heterogeneity within these grass-dominated areas likely affects the validation results at this site (see section 4). GPS reflections from the riparian corridor in the northeast portion of the maximum NMRI footprint are not received by the antenna. However, the riparian vegetation does affect the NDVI data we use for comparison purposes.

Vegetation heterogeneity at P049 is related to topography (Figure 2). At P049, both the near-antenna reflection zone and the two hotspots to the south of the antenna are in areas almost exclusively covered by grasses. Moderate livestock grazing occurs throughout the maximum sensing footprint at P049. The effects of grazing on our results are discussed below. Vegetation at P719 is the most uniform of all the sites (Figure 2). The antenna is surrounded by uniform grassland, with the exception of some small shrubs and bare soil areas below the break in slope to the west of the antenna.

2.3 In situ data collection

During the 2012 growing season vegetation was sampled at roughly biweekly intervals. The sites were visited either 11 or 12 times, depending upon sampling constraints, for a total of 46 site

visits. Twelve random locations were selected for each site visit. All azimuths were included in the random selection. Only distances between 30 and 100 m from the antenna were used. Samples were not taken closer to the antenna to minimize effects of foot travel and sampling near the antenna. Even though the maximum footprint size is 300 m, samples were not taken from more than 100 m from the antenna to minimize the time required to walk between the sample locations. Locations were selected without replacement, to prevent any one quadrant from being sampled more than once over the course of the growing season.

At each sample location, all aboveground plant material (including standing litter) within twelve 50 x 50 cm randomly selected quadrats was clipped and bagged. All samples were weighed immediately after clipping, subsequently oven-dried for two days at 60 deg C, and reweighed. Mass of the oven-dried vegetation will be referred to as biomass, converted to kg m^{-2} based on quadrat size. VWC is equal to the mass loss from oven-drying and also converted to kg m^{-2} . The mean and standard deviation of biomass and VWC were calculated for each of the site visits. The Relative Water Content (RWC) from each quadrat was calculated as VWC divided by the mass measured in the field (i.e. the portion of the total mass that was water), which differs from definitions of RWC based on turgid mass (e.g., [17]).

Vegetation height was measured by estimating the 90th percentile height of green vegetation in each quadrat. Both the green and brown 90th percentile vegetation heights were recorded after the onset of senescence. Distinguishing between green and brown vegetation is subjective as the transition between active and senesced vegetation is gradual. We tried to make this determination as consistent as possible by having a single person complete all vegetation surveys. On most survey dates, one or two of the 12 sample quadrats had no green vegetation at P719. Due to the

absence of green vegetation in some quadrats at P719, the median (not mean) green vegetation height for each site visit was calculated.

2.4 NMRI and NDVI data

GPS data: A detailed description of how the GPS data are processed to yield NMRI can be found in Paper I, so only a brief description is provided here. The following steps are carried out at each site. First, daily values of MP_{1rms} are extracted from standard archived GPS files. MP_{1rms} records are filtered for snow and outliers caused by rain. The rain clearing produces gaps in the NMRI record. These were eliminated using a 7-day median centered on the observation day. Without gap-filling, we would have had to exclude data from 7 of the 46 field surveys.

At each site, NMRI is calculated by normalizing the daily MP_{1rms} values using the average of the highest 5% individual MP_{1rms} values (equation 10, Paper I). This normalization adjusts to first order the effect from terrain and surface roughness. The highest 5% of observations provides a representative MP_{1rms} value for times when there is a minimum amount of vegetation. If only the maximum MP_{1rms} value was used, instead of the highest 5%, the normalization would be sensitive to outliers. Using a greater portion of the individual MP_{1rms} values (e.g., 10%) has a negligible effect on the NMRI time series, yielding a slight increase in all NMRI values. Importantly, the seasonal fluctuations and site-to-site differences in NMRI are effectively unchanged.

NDVI: We use MOD13 16-day 250 m MODIS NDVI data for comparison to NMRI. NDVI values were not used from intervals when the NMRI records had no data due to snow clearing. The NDVI data are presented to provide the reader with a standard frame of reference, not to

evaluate the relative merit of the two indices. In the 16-day dataset, NDVI values are not available on most of the field sampling dates. We linearly interpolated the NDVI values from the two closest NDVI observations that spanned the sampling day. This interpolation was completed using the actual day of the NDVI observations, not the midpoint of the 16-day NDVI window.

3. Results

3.1 Precipitation and remote sensing indices, climatology and 2012

We first discuss variations in precipitation, NMRI, and NDVI at the four sites. We describe the typical seasonal fluctuations using data from 2007-2012, the period of record of the GPS data. This summary is intended to put our field validation in perspective. Then, we focus on the conditions during the 2012 growing season used for validation.

The annual total and timing of precipitation in 2012 was not similar to climatology. Total annual precipitation was only near normal at P046. At the other three sites, annual precipitation was approximately 20% below the long-term average according to both NLDAS and PRISM datasets (Table 1). At these three sites, precipitation was near normal through March, but was roughly half the normal amount during most of the growing season (Figure 3). During July and August, the U.S. Drought Monitor conditions were “moderate” to “severe” at these sites (<http://droughtmonitor.unl.edu/monitor.html>). Summer precipitation was also below normal at P046, but drought conditions never reached the least-severe rating of “moderate”.

Next we characterize seasonal fluctuations in vegetation based on NDVI records. At each site, NDVI exhibits a strong annual cycle with a peak around June 1. The peak value is approximately

0.65 at P046, P048, and P049. At these three sites, the NDVI annual cycle changes little from year to year, including the 2012 drought year. The NDVI time series at P719 differs in two ways. First, the annual peak value is lower (0.45), which is consistent with this site receiving the least precipitation (Table 1). Second, there are more obvious year-to-year differences in the NDVI seasonal cycle. For example, the maximum NDVI in 2012 was only 0.05 above the non-growing season values. Below, we show that this is consistent with *in situ* observations of vegetation growth.

Seasonal variations of NMRI are evident at all four sites (Figure 3). Compared to the 16-day NDVI product, the daily NMRI data provides a high-resolution depiction of seasonal fluctuations. NMRI increases each spring to a peak around June 1, and subsequently decreases throughout the summer. The seasonal cycle is similar from year-to-year, including the magnitude of the peak and the length and timing of the period with high values. The data gap each winter is the result of the snow-clearing described in Part I. Additional outlier clearing has removed most of the noise in the record, leaving primarily the low-frequency variations consistent with seasonal vegetation growth and senescence. Below, we show that these low-frequency variations are related to changes in VWC. Fluctuations on timescales of days are absent from the NMRI time series. This suggests changes in near surface soil moisture associated with wetting-drying cycles have little effect on NMRI, at least during the growing season at the four sites studied here. As was the case with NDVI, the NMRI record from P719 is different from the other three sites. The maximum value is much lower and there is almost no peak during the 2012 growing season. It is clear from Figure 3 that NMRI and NDVI are highly correlated at the four Montana sites. This is discussed in more detail below (Section 3.3).

3.2 In situ observations of vegetation growth

Vegetation height and phenology

Phenological observations and height measurements show that the timing of vegetation growth was similar at the four sites. There was a gradual increase in vegetation height through the spring (Figure 4). The maximum vegetation height (35 cm) was measured on July 1-2 at P049 and P046. The peak height was reached three weeks earlier at P048 (30 cm) and P719 (25 cm). Vegetation height remained nearly constant as the grasses senesced. In some cases, greater heights were measured later in the season (e.g., August 10 at P049 and P046). These values are due to sampling variability. A second period of growth was not observed. Little or no green vegetation could be found by mid-August at P049 and P046. The onset of senescence was earlier and more rapid at P048, where little green vegetation was noted by mid-July. The last sampling date on which green vegetation was observed is shown in Figure 4.

VWC and biomass

Biomass varied little throughout the growing season (Figure 4). Nearly all measured values were between 0.1 and 0.15 kg m⁻². There were no obvious increases in biomass during the portion of the summer when vegetation height and NDVI were greatest. This may be due in part to grazing at P048 and P049. It may also be related to below-normal growth in 2012, such that new growth was largely balanced by loss of standing litter. Biomass was lowest at P719, where most values were below 0.1 kg m⁻².

In contrast, there were clear seasonal changes in vegetation water content (VWC). At P046, P048, and P049, VWC increased to 0.2-0.3 kg m⁻² in late June and early July, and quickly decreased thereafter. VWC remained nearly constant at 0.1 kg m⁻² for the remainder of the

sampling period. The seasonal fluctuations in VWC were associated with changes in relative water content (RWC), not increases in biomass at a constant RWC. Figure 5 shows the strong correlation between VWC and RWC. Across all sampling dates and sites, RWC increases from 0.4 to 0.7 as VWC increases from 0.1 to 0.3 kg m⁻². There were limited or no measurable changes in VWC at P719, where values were always approximately 0.1 kg m⁻².

3.3 Relationship between biophysical properties and NMRI, MP₁rms, and NDVI

We now describe the relationship between NMRI and *in situ* data at each site. A positive, linear relationship exists between NMRI and VWC at each of the four sites (Table 2, Figure 6a). A corresponding relationship exists between MP₁rms and VWC at each site, given the time-invariant scaling factor used to convert MP₁rms to NMRI at each site (Figure 6b). Our comparison is based on only 11 or 12 sampling points at each site. In addition, there is noise in both the *in situ* and NMRI (and MP₁rms) data. Additional data would be necessary to further refine estimates of correlation between remote sensing metrics and VWC on a site-by-site basis. This is not the case for the cross-site analysis described in Section 3.4.

The VWC-NMRI relationship is strongest at P046 and P048, the two sites with the greatest seasonal range in both variables. The relationship is not as clear at P049 and P719. Due to the drought in 2012, the seasonal cycle of NMRI at P719 was minimal compared to years with normal rainfall (Figure 3). We expect that the seasonal cycle of VWC was similarly affected. Therefore, the absence of a strong correlation in 2012 indicates little about the nature of the VWC-NMRI relationship at P719. Clear seasonal fluctuations in both NMRI and VWC were measured at P049, but the NMRI-VWC relationship was not as strong as that found for P046 and P048. The range of NMRI is less at P049 than at P046 and P048, but the high-frequency NMRI

variations unrelated to vegetation growth are not (Figure 4). Smoothing the NMRI data to minimize the effects of this noise increases r^2 by ~ 0.05 at P049, and by a similar amount at P048.

A positive linear relationship also exists between NDVI and VWC at all four sites (Table 2, Figure 6d). This suggests that greenness and VWC covary throughout the season, not that vegetation water directly affects NDVI. NMRI and NDVI are also strongly correlated. Using data from only the 11 or 12 sampling dates, r^2 between NMRI and NDVI is above 0.7 at all four sites. This is surprisingly high considering that the NDVI footprint includes trees and shrubs at three of the sites (Figure 2). In addition, the NDVI data are linearly interpolated from the observation day used in each 16-day window (Figure 4). This interpolation extends over intervals of nearly a month when consecutive NDVI observations are from the beginning and end of 16-day windows. The relationship between NMRI and NDVI is discussed further in Section 3.5.

The relationships between NMRI and the *in situ* observations of height and biomass are not as clear (Table 2, Figure 6c). A significant linear relationship does not exist between NMRI and vegetation height, except at P046 where a weak relationship exists. NMRI and biomass are weakly correlated at P048 and P049, but not at the other sites. Similarly, the observed relationships between NDVI and height and biomass are not strong, especially when compared to that seen for NMRI and VWC.

3.4 Cross-site comparison

The cross-site relationships between NMRI and the *in situ* observations are now summarized. This comparison provides information on whether or not biophysical parameters can be predicted from NMRI data at a site, using a relationship measured elsewhere in the same ecosystem. A positive, linear relationship exists between NMRI and VWC ($r^2 = 0.71$) (Figure 6a, Table 2).

The observed relationship exists because of the differences between sites and the seasonal variations at each site. The lowest VWC and NMRI values are from P719 and the highest are from P046. Seasonal variations yield data pairs that fall between these end members. The two most obvious outliers are from P048. These outliers are from the two sampling visits following the timing of peak VWC, when NMRI remained high but VWC dropped dramatically. We expect that these outliers are due to spatial heterogeneity at the site (Section 4).

A positive, linear relationship also exists between NDVI and VWC (Table 2, Figure 6d). However, NDVI remains constant for VWC values greater than 0.2 kg m^{-2} , so a linear relationship does not provide a good fit to the data. The coefficient of determination is slightly lower ($r^2 = 0.68$) than calculated for NMRI and VWC. There is a weak relationship between both indices and biomass, and no relationship between the indices and vegetation height (Figure 6, Table 2).

3.5 Importance of normalization

NMRI is normalized using the highest 5% MP_{1rms} values observed at each site (Paper I). This normalization adjusts the record of microwave scattering from each site to account for differences in terrain. Figure 6 shows the importance of normalizing the MP_{1rms} data. At each site, there is a clear relationship between MP_{1rms} and VWC. However, there is no relationship between MP_{1rms} and VWC when the four sites are considered together (Figure 6b). Only after normalization does a cross-site relationship emerge.

The value of normalizing MP_{1rms} is further demonstrated by analyzing data from eight additional GPS sites in Montana. Together with the validation sites, these twelve sites are all the PBO sites in Montana that are classified as grassland at both the NMRI and NDVI scale. There

are no *in situ* measurements of vegetation at the eight additional sites. Therefore, we use NDVI as a proxy for vegetation status. At each site, MP_{1rms} and NDVI are linearly related (Figure 7 left). This can be seen by the series of points from individual sites that tend to fall along a coherent line. However, there is no consistent relationship between MP_{1rms} and NDVI across the twelve sites. After normalization, a strong positive correlation is apparent (Figure 7 right). The NMRI-NDVI relationship is surprisingly consistent across the region, considering the extensive differences between the two indices.

4. Discussion

The *in situ* observations from Montana grassland sites show that NMRI is a predictor of vegetation water content (VWC). At each site, a positive linear relationship exists between VWC and NMRI. The slopes and strengths of these site-specific relationships are not well constrained, given the number of data points and noise in both the *in situ* observations and NMRI data. However, when data are combined across the validation sites, it is clear that the linear VWC-NMRI relationship is consistent across the region. This suggests that VWC could be predicted from NMRI at sites without *in situ* observations, as long as vegetation and climate are similar.

The data presented here shows that NMRI does not vary consistently with vegetation height or biomass. In Small et al. [1] MP_{1rms} varied with both vegetation height and VWC at two agricultural sites. Each site was considered independently, so the variations in MP_{1rms} are linearly related to variations of NMRI. We expect that these contrasting results are related to differences in plant-water dynamics in the two ecosystems. Here, the seasonal changes in VWC are linked to variations in RWC (Figure 5), not to changes in vegetation height or biomass. In contrast, the RWC of vegetation at the agricultural ecosystems is relatively constant, and VWC

scales consistently with plant size. Therefore, the MP_{1rms} -vegetation height link observed by Small et al. [1] was likely an outcome of the covariance between VWC and height in the agricultural ecosystems, not because vegetation height directly impacts NMRI.

These results presented above are a first attempt to validate NMRI for VWC retrievals in non-agricultural ecosystems. These results are from a single growing season during which rainfall was below normal at three of the four sites. The VWC-NMRI relationship could be different in years with above-average rainfall when biomass and vegetation height are presumably greater. We expect that the VWC-NMRI relationship observed in Montana grasslands is not directly transferrable to other ecosystems, as is the case for relationships between optical indices and biophysical parameters [18]. Thus, additional validation data should be collected in other ecosystems. In particular, collocated *in situ* observations and NMRI data from ecosystems with higher VWC are needed to assess if NMRI saturates at high values of VWC, as is the case for other remote sensing indices.

The results presented here demonstrate that the normalization procedure used to scale the MP_{1rms} data is effective. After MP_{1rms} data are normalized, the VWC-NMRI relationship is consistent across the four validation sites (Figure 6). The data from the eight additional sites show that the procedure is effective across the range of terrain that exists in Montana grasslands. The flattest site included in the analysis is P051, which is located at the airport in Billings, Montana. The MP_{1rms} values from this site are the lowest of the twelve sites considered (the asterisks in Figure 7 left). After normalization, even the NMRI values from this extreme site are consistent with those from the entire population (Figure 7 right).

Like other remote sensing techniques, NMRI is affected by heterogeneity within the sampling footprint. The maximum radius of the sampled footprint is 300 m. However, the portion of this maximum-possible sensing zone that produces reflections that make it to the antenna depends on topography. At flat sites, the signal comes primarily from the near-antenna reflection zone (~20 m radius). The ‘sampled area’ grows as topography around the antenna becomes more complex. The actual areas sampled depend on interactions between terrain and the GPS signals. In addition, a signal’s contribution to the site-level MP_{rms} , and thus NMRI, increases linearly with distance sampled (see equation 4 in Paper I). The result is that some areas within the footprint act as ‘hot spots’ that dominate the NMRI signal. If the vegetation in these hotspots is different than the ‘average vegetation’ around the antenna, then the NMRI record will not be indicative of the average conditions across the sensing footprint.

We suspect that spatial heterogeneity affected the validation results presented above. A clear example comes from P048. A hot spot ~140 m northwest of the antenna has a strong influence on the NMRI record (Figure 2b). The vegetation in this hotspot is different than in other areas around the antenna. There are some shrubs in the hot spot, but this difference is likely minor as the area is still dominated by grasses. More importantly, the grasses in the hot spot remain active longer into the summer than in other parts of the footprint. This was observed during field visits in 2012 and can be seen in the Google Earth image. We suspect that this happens because the soil in the hot spot is relatively wet. The aspect in this part of the sampling footprint is northward, minimizing evapotranspiration. The area is also at a break in slope that could concentrate soil water. We suspect this is the source of the two outliers in Figure 6. Based on the average of field measurements from around the antenna, VWC dropped quickly following the peak in late June (Figure 4). NMRI dropped more slowly, likely because vegetation in the hot

spot remained active longer. If this interpretation is correct, it suggests that the effects of topography on NMRI are complex. Topography determines areas within the footprint that are hot spots. At the same time, topography affects both the composition of the vegetation and its seasonal evolution.

NDVI is almost as good of a predictor of VWC as NMRI across the validation sites (Table 2), although the NDVI-VWC relationship is not linear across the range of observations (Figure 6d). Similar results have been found in other validation studies: NDVI provides predictions of VWC that are similar to metrics designed specifically to sense water [9]. As mentioned in these other studies, the observed NDVI-VWC is not due to the direct effects of vegetation water on NDVI, but instead due to the correlation that exists between greenness and VWC. NMRI and NDVI are highly correlated at the validation sites, and at the eight other grassland sites in Montana shown in Figure 7. This is not the case at many other sites in the GPS network. For example, the start-of-season increase in NDVI precedes that of NMRI by a month or longer at many sites in California [19].

Even at sites where NMRI and NDVI are highly correlated, NMRI data provides important and unique information regarding plant phenology and the response to extreme events such as drought. A well-known shortcoming of NDVI and other optical indices is data loss due to clouds. Standard NDVI datasets, such as the MOD13 16-day 250 m MODIS product used here, have long repeat intervals. For example, there are only four NDVI data points during the entire growth interval at P049. In contrast, NMRI is calculated daily, and only a small fraction of the data is excluded by the data-cleaning process. For example, only three data points were removed from the NMRI record during the growth interval at P049. Therefore, the NMRI data provide a

more complete record of the timing of plant growth and senescence, particularly in ecosystems with rapid dynamics.

Future research should be focused on several key aspects of using NMRI to monitor vegetation. The relationship between NMRI and NDVI in different ecosystems and climates should be explored. Many GPS sites have more complex topography than those used here, and a further evaluation of the current normalization is needed. Finally, the effects of soil moisture, surface roughness, and other environmental factors on NMRI should be quantified. Multi-year NMRI time series, as well as various ancillary data streams, are available for 330 sites in the western U.S. (<http://xenon.colorado.edu/portal/>). These data can be used for these analyses across a broad range of environmental conditions.

5. Conclusions

NMRI, MP₁rms, and NDVI were compared to *in situ* vegetation observations at four grassland PBO sites in Montana. Conclusions from this validation effort are as follows:

1. A significant linear relationship exists between MP₁rms and VWC at each site; however, this relationship is not consistent across the four sites.
2. Once MP₁rms is normalized to adjust for terrain effects, a consistent relationship exists between NMRI and VWC across the four validation sites. Relationships between biomass or vegetation height and NMRI are comparatively weak. NDVI does vary significantly with VWC, although a linear relationship does not provide the best fit.

3. The normalization procedure is effective across the twelve grassland PBO sites in Montana. After MP_{1rms} is converted to NMRI, there is a consistent linear relationship between NMRI and NDVI across all twelve sites.

6. Acknowledgements

This research was funded by EAR-0948957, AGS-0935725, EAR-1144221, and NNX12AK21G. At UNAVCO we thank Lou Estey, Fran Boler, and Karl Feaux. John Braun, Felipe Nievinski, Ethan Gutmann, and Praveen Vikram provided assistance for this project. Some of this material is based on data, equipment, and engineering services provided by the Plate Boundary Observatory operated by UNAVCO for EarthScope and supported by NSF (EAR-0350028 and EAR-0732947). All GPS data used in this study are archived at UNAVCO. NMRI time series can be downloaded from <http://xenon.colorado.edu/portal>.

7. References Cited

- [1] E. E. Small, K. M. Larson, and J. J. Braun, "Sensing vegetation growth with reflected GPS signals," *Geophysical Research Letters*, vol. 37, no. L12401, p. 5, Jun. 2010.
- [2] L. Estey and C. Meertens, "TEQC: The multi-purpose toolkit for GPS/GLONASS data," *GPS Solutions*, vol. 3, no. 1, pp. 42–49, 1999.
- [3] A. R. Huete, "A soil-adjusted vegetation index (SAVI)," *Remote Sensing of Environment*, vol. 25, no. 3, pp. 295–309, Aug. 1988.
- [4] C. J. Tucker, "Red and photographic infrared linear combinations for monitoring vegetation," *Remote Sensing of Environment*, vol. 8, no. 2, pp. 127–150, May 1979.
- [5] R. B. Myneni, F. G. Hall, P. J. Sellers, and A. L. Marshak, "The interpretation of spectral vegetation indexes," *IEEE Transactions on Geoscience and Remote Sensing*, vol. 33, no. 2, pp. 481–486, 1995.
- [6] J. M. Paruelo, H. E. Epstein, W. K. Lauenroth, and I. C. Burke, "ANPP estimates from NDVI for the central grassland region of the United States," *Ecology*, vol. 78, no. 3, pp. 953–958, Apr. 1997.
- [7] A. Richardson, J. Jenkins, B. Braswell, D. Hollinger, S. Ollinger, and M.-L. Smith, "Use of digital webcam images to track spring green-up in a deciduous broadleaf forest," *Oecologia*, vol. 152, no. 2, pp. 323–334, 2007.
- [8] P. J. Kramer and J. S. Boyer, *Water relations of plants and soils*. Academic Press, Inc., 1995, p. 495.
- [9] B. Gao, "NDWI—A normalized difference water index for remote sensing of vegetation liquid water from space," *Remote Sensing of Environment*, vol. 58, no. 3, pp. 257–266, Dec. 1996.
- [10] D. Chen, J. Huang, and T. J. Jackson, "Vegetation water content estimation for corn and soybeans using spectral indices derived from MODIS near- and short-wave infrared bands," *Remote Sensing of Environment*, vol. 98, no. 2–3, pp. 225–236, Oct. 2005.
- [11] F. T. Ulaby, R. K. Moore, and A. K. Fung, *Microwave Remote Sensing: Active and Passive, Vol III, from theory to applications*. Norwood, MA: Artech House Publishers, 1981, p. 2162.
- [12] Y. Kim, T. Jackson, R. Bindlish, H. Lee, and S. Hong, "Radar vegetation index for estimating the vegetation water content of rice and soybean," *IEEE Geoscience and Remote Sensing Letters*, vol. 9, no. 4, pp. 564–568, 2012.

- [13] T. R. Loveland, B. C. Reed, J. F. Brown, D. O. Ohlen, Z. Zhu, L. Yang, and J. W. Merchant, "Development of a global land cover characteristics database and IGBP DISCover from 1 km AVHRR data," *International Journal of Remote Sensing*, vol. 21, no. 6–7, pp. 1303–1330, Jan. 2000.
- [14] W. M. Jolly, R. Nemani, and S. W. Running, "A generalized, bioclimatic index to predict foliar phenology in response to climate," *Global Change Biology*, vol. 11, no. 4, pp. 619–632, Apr. 2005.
- [15] K. E. Mitchell, D. Lohmann, P. R. Houser, E. F. Wood, J. C. Schaake, A. Robock, B. A. Cosgrove, J. Sheffield, Q. Y. Duan, L. F. Luo, R. W. Higgins, R. T. Pinker, J. D. Tarpley, D. P. Lettenmaier, C. H. Marshall, J. K. Entin, M. Pan, W. Shi, V. Koren, J. Meng, B. H. Ramsay, and A. A. Bailey, "The multi-institution North American Land Data Assimilation System (NLDAS): Utilizing multiple GCIP products and partners in a continental distributed hydrological modeling system," *Journal of Geophysical Research*, vol. 109, no. D7, pp. 1–32, Apr. 2004.
- [16] C. Daly, R. P. Neilson, and D. L. Phillips, "A statistical-topographic model for mapping climatological precipitation over mountainous terrain," *Journal of Applied Meteorology*, vol. 33, no. 2, pp. 140–158, Feb. 1994.
- [17] J. Peñuelas, I. Filella, C. Biel, L. Serrano, and R. Savé, "The reflectance at the 950–970 nm region as an indicator of plant water status," *International Journal of Remote Sensing*, vol. 14, no. 10, pp. 1887–1905, Jul. 1993.
- [18] B. . Wylie, D. . Meyer, L. . Tieszen, and S. Mannel, "Satellite mapping of surface biophysical parameters at the biome scale over the North American grasslands," *Remote Sensing of Environment*, vol. 79, no. 2–3, pp. 266–278, Feb. 2002.
- [19] S. Evans, "Sensing vegetation growth and senescence with reflected GPS signals: active microwave detection of western North America phenology," University of Colorado, Boulder, 2013.

Figure and Table Captions

Figure 1. All Plate Boundary Observatory GPS sites in Montana classified as grassland. The four field validation sites are denoted by the filled circles. GPS and NDVI data were used from eight additional sites, denoted by open circles.

Figure 2. GoogleEarth images of field validation sites. GPS antenna is located at the center of the circles, which are marked according to distance in meters. The inner blue circle is the near-antenna reflection zone. The wedge is missing on the north side because no satellites rise or set in these azimuths. The other blue circles indicate reflection hot spots.

Figure 3. NMRI, yearly cumulative precipitation from NLDAS, and NDVI records for each site. The precipitation panel includes the cumulative amount for each year (red) and the 6-year average cumulative record (black).

Figure 4. NMRI, NDVI, and field observations of vegetation parameters during the 2012 growing season. Vegetation height is for green vegetation only; height is not plotted on sampling dates when only brown vegetation was observed. For clarity, legend is only shown in the P048 plots. NDVI is plotted on the day from the 16-day window when the data was recorded.

Figure 5. Relative water content (RWC) versus vegetation water content (VWC) for all sites and sampling dates. Color indicates site. Each point is the average from the 12 samples collected at each site visit.

Figure 6. Comparison of field observations of vegetation parameters with NMRI, MP_{1rms} , and NDVI. Color indicates site. Each point is the average from the 12 samples collected at each site

visit. (A) VWC versus NMRI; (B) VWC versus MP_{1rms} ; (C) Green vegetation height versus NMRI; and (D) VWC versus NDVI.

Figure 7. Left: Comparison of NDVI and MP_{1rms} from 12 PBO grassland sites in Montana. Data represent the full period of record in Figure 3 (2007-2012). Each site has a different symbol. Right: Same for comparison between NDVI and NMRI.

Table 1. Validation site information. Mean annual precipitation (mm) and 2012 precipitation (% of normal) as estimated from PRISM and NLDAS at the location of the sites.

			NLDAS Precipitation		PRISM Precipitation	
Site	Lat/Long	Elevation (m)	Mean annual (mm)	2012 (% of normal)	Mean annual (mm)	2012 (% of normal)
P046	47.03 / -113.33	1291	506	95.2	426	95.2
P048	45.65 / -111.204	1493	443	74.0	429	75.6
P049	47.35 / -110.90	1186	521	73.1	424	79.8
P719	45.21 / -111.79	1706	428	84.1	390	83

Table 2. Coefficient of determination (r^2) between in situ observations and NMRI and NDVI.

Values are shown for each site separately, and considering data from all four sites together (last row). Bold indicates a linear relationship is significant ($p < 0.05$).

	NMRI			NDVI		
Site	Height	Biomass	VWC	Height	Biomass	VWC
P046	0.37	0.14	0.87	0.00	0.24	0.70
P048	0.11	0.61	0.58	0.03	0.70	0.79
P049	0.29	0.60	0.48	0.00	0.35	0.85
P719	0.00	0.11	0.46	0.47	0.38	0.49
All	0.16	0.31	0.71	0.00	0.40	0.68

Figure 1. All Plate Boundary Observatory GPS sites in Montana classified as grassland. The four field validation sites are denoted by the filled circles. GPS and NDVI data were used from eight additional sites, denoted by open circles.

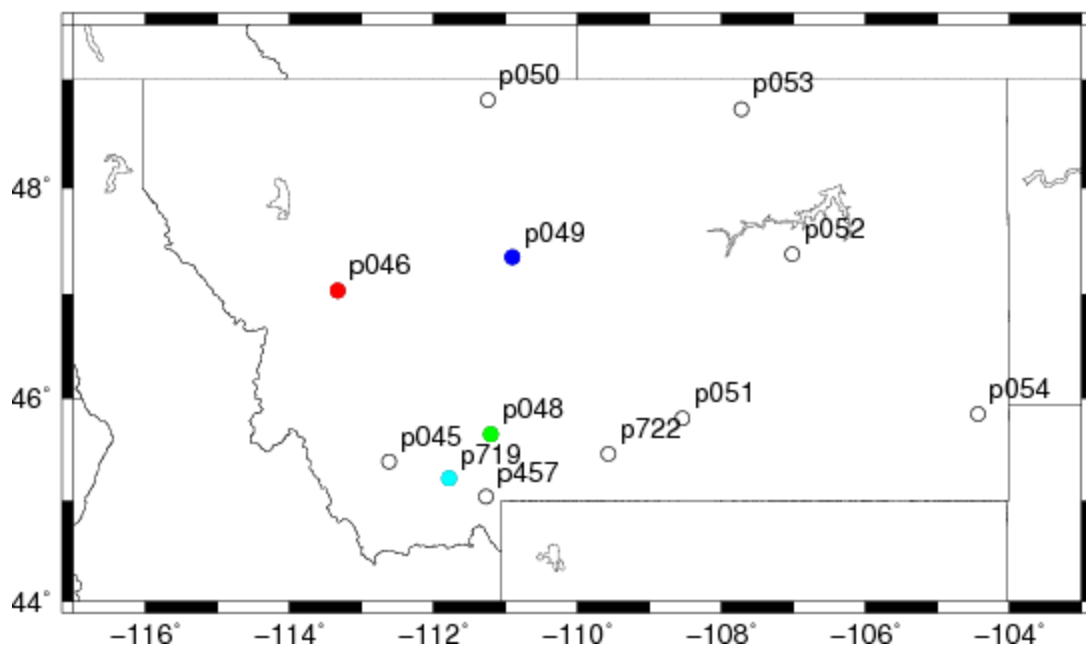


Figure 2. GoogleEarth images of field validation sites. GPS antenna is located at the center of the circles, which are marked according to distance in meters. The inner blue circle is the near-antenna reflection zone. The wedge is missing on the north side because no satellites rise or set in these azimuths. The other blue circles indicate reflection hot spots.

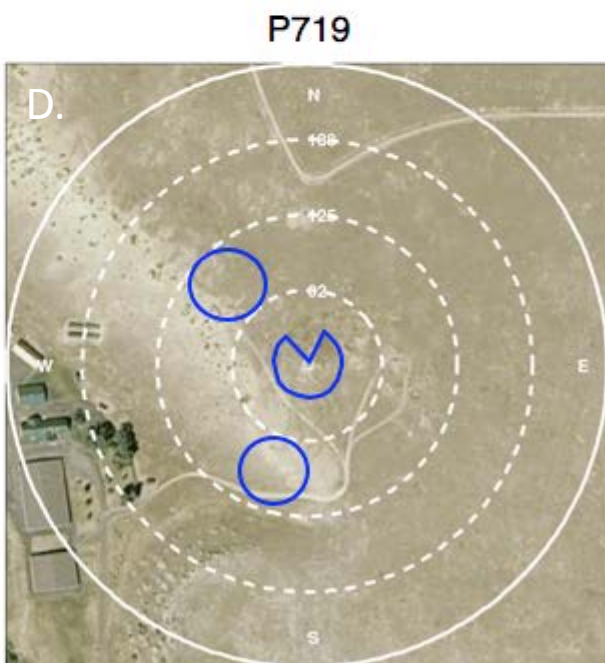
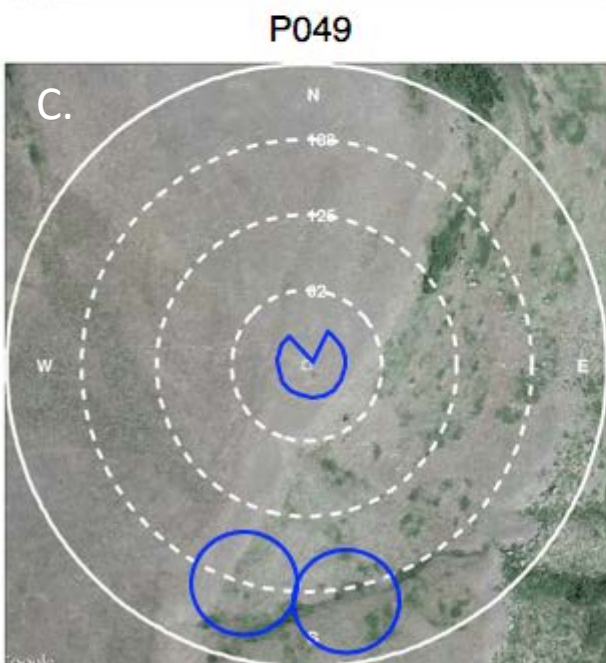
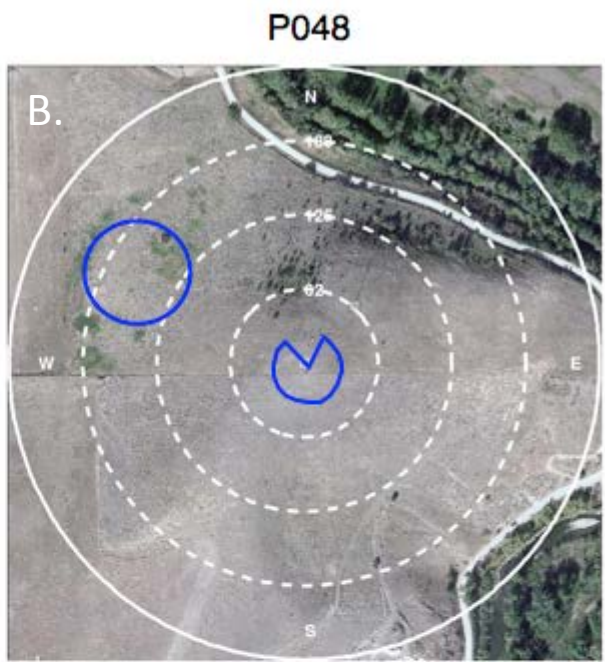
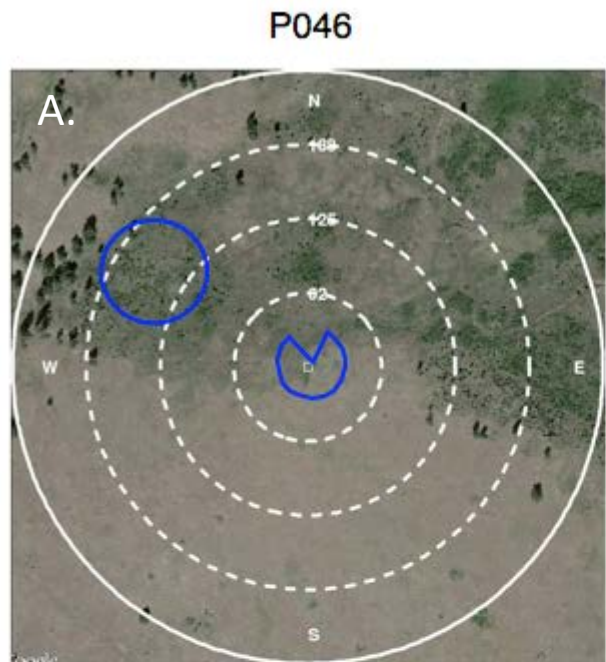


Figure 3. NMRI, yearly cumulative precipitation from NLDAS, and NDVI records for each site. The precipitation panel includes the cumulative amount for each year (red) and the 6-year average cumulative record (black).

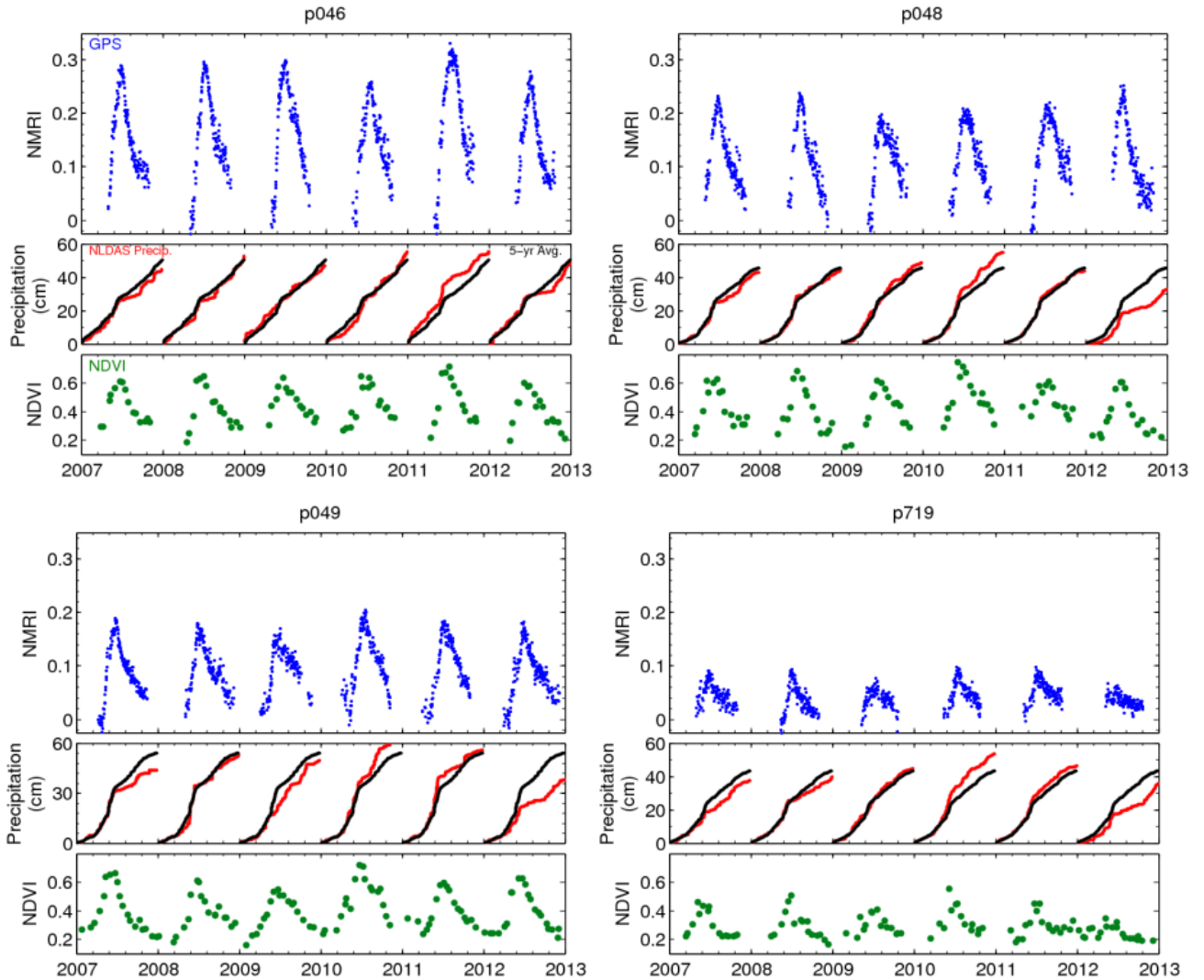


Figure 4. NMRI, NDVI, and field observations of vegetation parameters during the 2012 growing season. Vegetation height is for green vegetation only; height is not plotted on sampling dates when only brown vegetation was observed. For clarity, legend is only shown in the P048 plots. NDVI is plotted on the day from the 16-day window when the data was recorded.

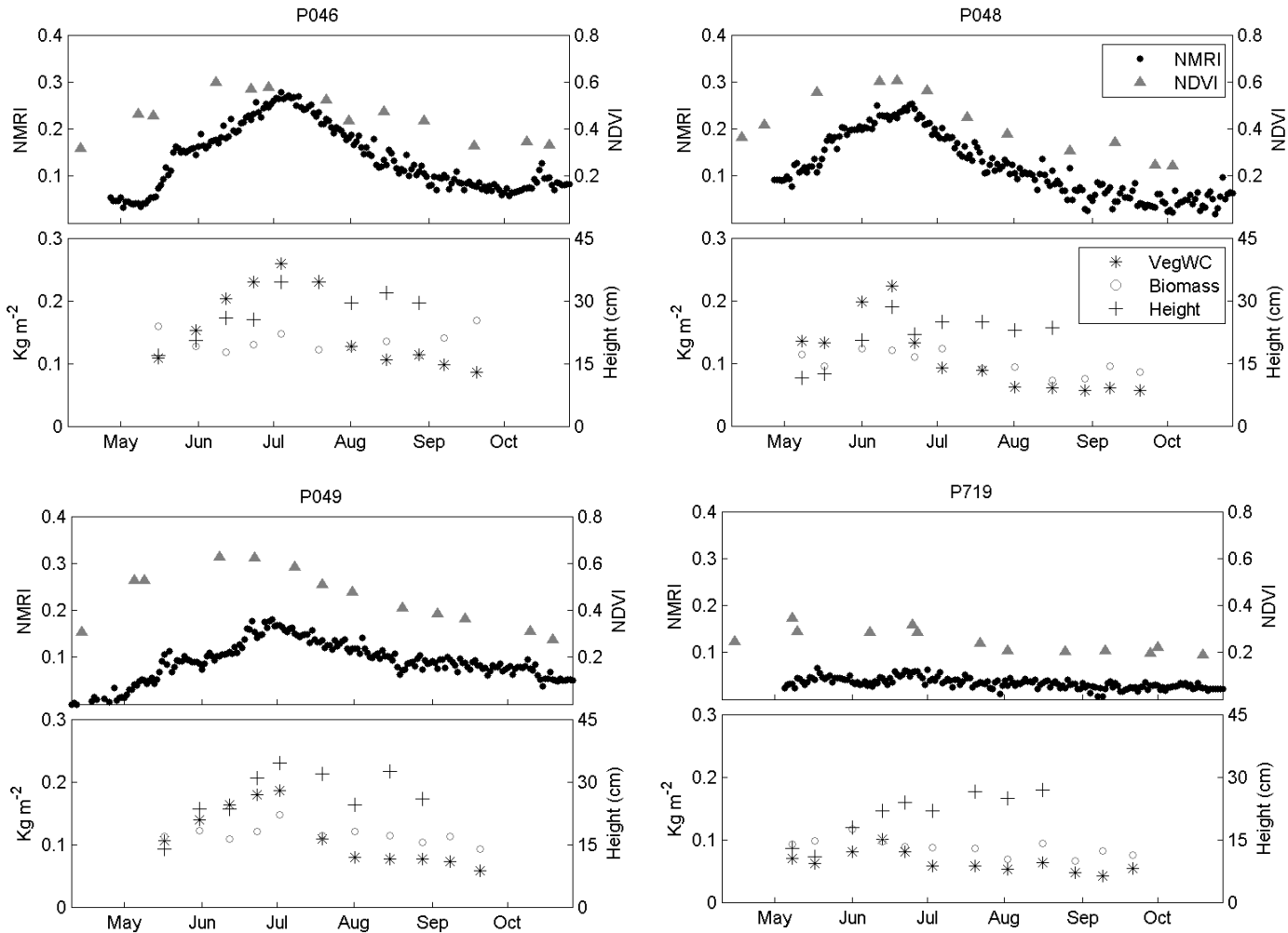


Figure 5. Relative water content (RWC) versus vegetation water content (VWC) for all sites and sampling dates. Color indicates site. Each point is the average from the 12 samples collected at each site visit.

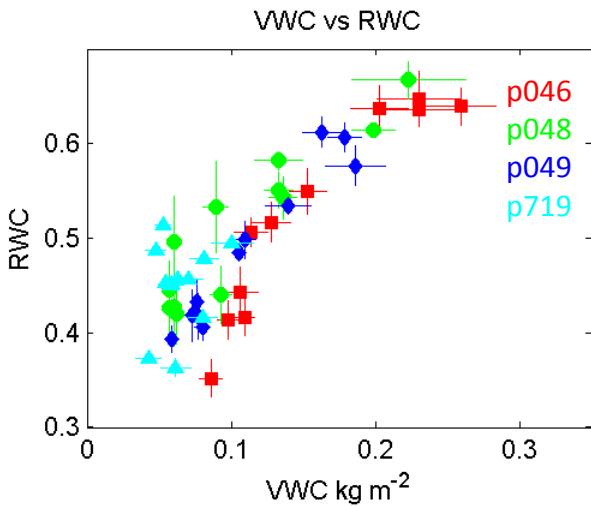


Figure 6. Comparison of field observations of vegetation parameters with NMRI, MP_1 rms, and NDVI. Color indicates site. Each point is the average from the 12 samples collected at each site visit. (A) VWC versus NMRI; (B) VWC versus MP_1 rms; (C) Green vegetation height versus NMRI; and (D) VWC versus NDVI.

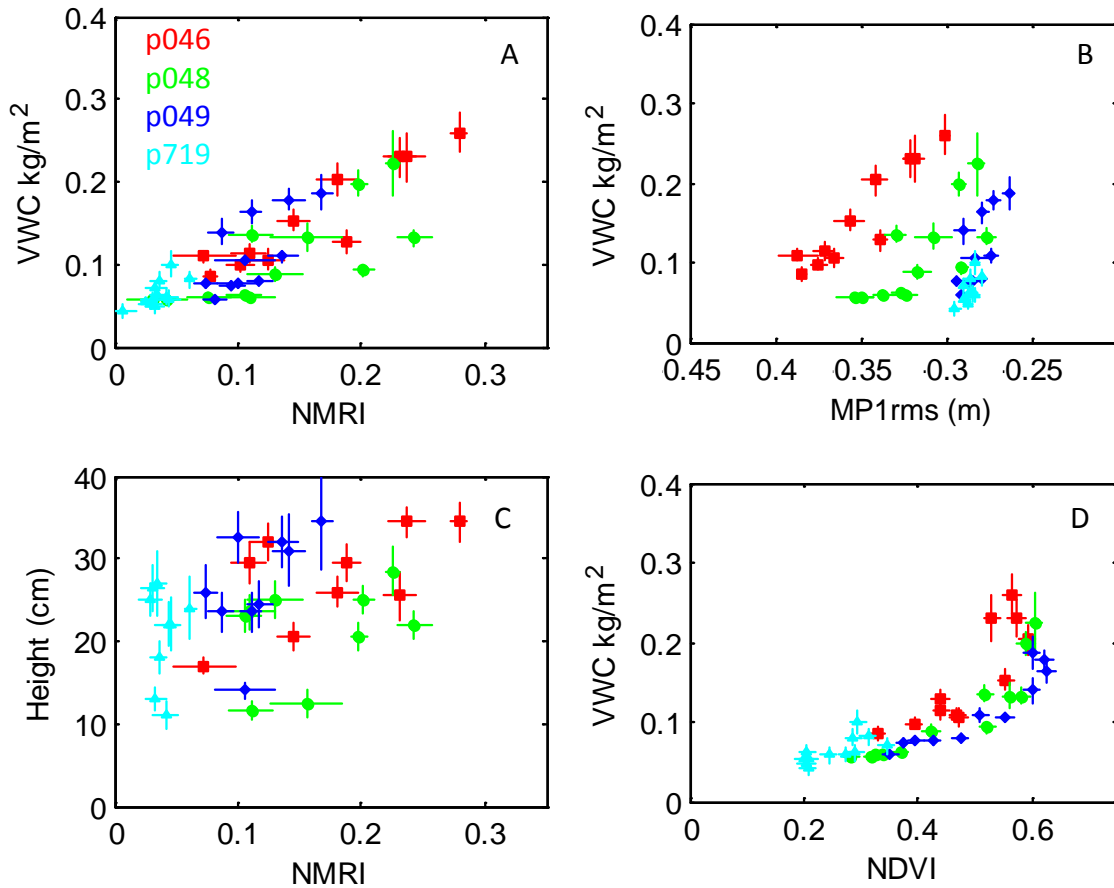


Figure 7. Left: Comparison of NDVI and MP₁rms from 12 PBO grassland sites in Montana. Data represent the full period of record in Figure 3 (2007-2012). Each site has a different symbol. Right: Same for comparison between NDVI and NMRI.

